**Influences of coral genotype and seawater $pCO_2$ on skeletal Ba/Ca and Mg/Ca in cultured massive *Porites* spp. corals**

N. Allison[*1], C. Cole[1], C. Hintz[2], K. Hintz[3], A.A. Finch[1]

**Corresponding author, email:* na9@st-andrews.ac.uk*; telephone: +44 1344 463940*
*[1] School of Earth and Environmental Sciences, University of St. Andrews, St. Andrews KY16 9AL, UK*
*[2] Department of Marine and Environmental Sciences, Savannah State University, Savannah, GA USA*
*[3] Department of Electrical and Computer Engineering, George Mason University, Fairfax, VA, USA*
*[4] Edinburgh Ion Microprobe Facility, Grant Institute, University of Edinburgh, Edinburgh EH9 3JW, UK*

**Abstract**

Coral skeletal Ba/Ca is a proxy for seawater Ba/Ca, used to infer oceanic upwelling and terrigenous runoff while [$Mg^{2+}$] is implicated in the control of coral biomineralisation. We cultured large individuals (>12 cm diameter) of 3 genotypes of massive adult *Porites* spp. corals over a range of seawater $pCO_2$ to test how atmospheric $CO_2$ variations affect skeletal Ba/Ca and Mg/Ca. We identified the skeleton deposited after a 5 month acclimation period and analysed the skeletal Ba/Ca and Mg/Ca by secondary ion mass spectrometry. Skeletal Mg/Ca varies significantly between some duplicate colonies of the same coral genotype hampering identification of genotype and seawater $pCO_2$ effects. Coral aragonite:seawater Ba/Ca partition coefficients ($K_D$ Ba/Ca) do not vary significantly between duplicate colonies of the same coral genotype. We observe large variations in $K_D$ Ba/Ca between different massive *Porites* spp. coral genotypes irrespective of seawater $pCO_2$. These variations do not correlate with coral calcification, photosynthesis or respiration rates or with skeletal $K_D$ Mg/Ca or $K_D$ Sr/Ca. Seawater $pCO_2$ does not significantly affect $K_D$ Ba/Ca in 2 genotypes but $K_D$ Ba/Ca is significantly higher at 750 µatm seawater $pCO_2$ than at 180 µatm in 1 *P. lutea* genotype. Genotype specific variations in $K_D$ Ba/Ca between different *Porites* spp. could yield large errors (~250%) in reconstructions of seawater Ba when comparing Ba/Ca between corals. Analysis of fossil coral specimens deposited at low seawater $pCO_2$, may underestimate past seawater Ba/Ca and ocean upwelling/freshwater inputs when compared with modern specimens but the effect is small in comparison with the observed difference between coral genotypes.

**Keywords:** Calcification, photosynthesis, respiration, $K_D$ Ba/Ca, $K_D$ Mg/Ca, coral

## 1. Introduction

Coral skeletal Ba/Ca correlates well with seawater Ba/Ca (Lavigne et al., 2016) and coral skeletal Ba/Ca records have been used to infer past seawater Ba concentrations, [Ba]. Dissolved oceanic Ba typically exhibits a nutrient-type vertical profile and is depleted in surface waters and regenerated at depth (Chan 1977). Both oceanic upwelling and terrigenous runoff are assumed to increase surface seawater [Ba] (Walther et al., 2013) and coral skeletal Ba/Ca records have been used to reconstruct past ocean circulation (Lea et al. 1989, Montaggioni et al., 2006) and/or local rainfall and freshwater inputs (Sinclair and McCulloch 2004; Walther et al., 2013). The application of the coral skeletal Ba/Ca proxy assumes that other biological and environmental factors either have no significant effect on skeletal Ba/Ca or can be corrected for e.g. temperature (Gonneea et al., 2017). However skeletal Ba/Ca was significantly higher (by ~20%) in a slow-growing *Porites lobata* field specimen compared to an adjacent faster growing individual (Allison and Finch 2007)

and also varied significantly between individual juvenile *Favia fragum* colonies grown in the same aquaria, independent of calcification rate (Gonneea et al. 2017). Other skeletal proxies e.g. Sr/Ca can be affected by coral calcification rate (de Villiers et al., 1994; de Villiers et al., 1995), coral species and genotype (de Villiers et al., 1995) and seawater $pCO_2$ (Cole et al., 2016).

Seawater $pCO_2$ is a potential complicating factor in interpreting fossil coral skeletal records. Before the preindustrial period, atmospheric $CO_2$ typically ranged from ~180 ppm (during glacial periods) to ~270 ppm (during interglacials) and was always significantly lower than during the present day (Petit et al., 1999). Seawater $pCO_2$ affects the dissolved inorganic carbon chemistry of the seawater derived calcification fluid used for aragonite formation (Venn et al., 2012) and this may affect trace element incorporation (e.g. Holcomb et al., 2016; Cole et al., 2016). All skeletal Ba/Ca:seawater Ba/Ca coral calibrations have used modern day corals (Lea et al., 1989; Lavigne et al., 2016; Gonneea et al., 2017) and may not be applicable to fossil specimens which grew under lower seawater $pCO_2$.

To improve our understanding of Ba incorporation in coral we cultured multiple genotypes of massive *Porites* spp. (the genus most commonly used for palaeoenvironmental reconstruction) over a range of seawater $pCO_2$, selecting concentrations that reflect present day conditions (~400 µatm) and values that are both lower and higher (180 and 750 µatm). Our range encompasses the likely concentration at the Last Glacial Maximum (Gattuso et al., 2009) and that projected to occur by the end of the present century (IPCC 2013). We acclimated the corals to altered seawater $pCO_2$ for 5 months, identified the skeleton deposited after this period by alizarin red staining (Cole et al., 2016) and analysed its Ba/Ca and Mg/Ca composition. $Mg^{2+}$ influences $CaCO_3$ precipitation (Falini et al., 2009; Tao et al., 2009; Addadi et al., 2003) and is implicated in the control of coral biomineralisation (Sancho-Tomas et al., 2014). We explore the impacts of seawater $pCO_2$ and coral genotype on skeletal Ba/Ca and we correlate both skeletal Ba/Ca and Mg/Ca with rates of key physiological processes (calcification, photosynthesis and respiration) measured during the experiment (Cole et al. 2018).

## 2. Methods

We tested the effect of variations in seawater $pCO_2$ on the skeletal incorporation of Mg and Ba in 3 genotypes of massive *Porites* spp. corals at 25°C. All corals were harvested by a commercial collector from the same reef site in Fiji and imported into the UK. We assume that coral heads collected from large, spatially separate (non-adjoining) colonies represent different coral genotypes. We cut multiple sub-colonies (each ≥12 cm in diameter) from heads collected from each genotype to enable the study of large individuals of the same genotype in each $pCO_2$ treatment. The physiological performance of small experimental coral colonies is not representative of larger colonies (Edmunds and Burgess, 2016). After sacrifice genotypes were identified to species level from surface skeletal morphology (Vernon, 2003). Two genotypes were identified as *P. lutea* and one as *P. murrayensis* (see Cole et al., 2016 for images of each coral). Two replicate colonies of the *P. murrayensis* genotype were cultured and analysed in 400 and 750 µatm seawater $pCO_2$. These corals have previously been analysed for Sr/Ca and full details of this and the culture system are provided in Cole et al., 2016. Briefly, corals were cultured in an aquarium system constructed of low $CO_2$ permeability materials and designed to control temperature, salinity and dissolved inorganic carbon (DIC) system parameters within narrow limits (Cole et al., 2016). Corals were housed in 21 l cast acrylic tanks, recirculated with seawater from high density polyethylene reservoirs containing ~900 litres of seawater bubbled with gas mixes set to reach the target seawater $pCO_2$ compositions. Corals were cultured at seawater $pCO_2$ of ~180 µatm (the $CO_2$ atmosphere during the last glacial maximum, Petit et al., 1999), ~400 µatm (the present day) and ~750 µatm (projected to occur by the end of the present century, IPCC 2013). Lighting was provided on a 12h light: 12h dark cycle such

that photosynthetically active radiation (PAR) intensity at coral depth was ~300 µmol photons $m^{-2}$ $s^{-1}$. Corals were fed weekly with rotifers.

After import into the aquarium, corals were maintained at ambient seawater $pCO_2$ conditions for 2 months, adjusted to treatment $pCO_2$ over another 2 months and then acclimated at the final treatment $pCO_2$ for 5 months, all at 25°C. Coral calcification rate is a potential control on coral skeletal Mg/Ca and Ba/Ca geochemistry (Allison and Finch, 2007) but the response of calcification to altered seawater $pCO_2$ can be affected by exposure duration (Castillo et al., 2014). Maintenance of control calcification rates during short $pCO_2$ exposures could be explained by catabolism of stored lipids which then become depleted during longer $pCO_2$ exposures (Castillo et al., 2014). The lipid reserves of massive *Porites lobata* field corals can sustain coral metabolic requirements under sub optimal growth conditions for >10 weeks (Spencer Davies 1991). Our acclimation times are much longer than this and it is unlikely that the response of the corals to altered seawater $pCO_2$ is affected by short term catabolism of any storage lipids.

At the end of the 5 month acclimation corals were incubated in 10 mg $l^{-1}$ alizarin red for 8 hours (whilst maintaining seawater $pCO_2$) to create a stain line in the skeleton (Cole et al., 2016). A 5 week experimental period followed in which calcification, respiration and net and gross photosynthesis were measured in each coral colony on 3 or 4 occasions (Cole et al., 2018). At the end of the experimental period the corals were sacrificed and immersed in 3-4% sodium hypochlorite solution for 24 h (to remove tissue). The skeletons were rinsed repeatedly in distilled water, dried and analysed by secondary ion mass spectrometry (SIMS).

### 2.1 Seawater chemistry

The reservoir seawater was ~80-85% fresh artificial seawater (Red Sea Salt, Red Sea Aquatics, UK) diluted with artificial seawater from a mixed coral/fish aquarium. ~10-15 l of seawater was usually removed from each reservoir each week (during removal of microalgae from the tank surfaces) and was replaced with fresh artificial seawater. No seawater replacement occurred during the 5 week experimental period. The total alkalinity, [Ca] and [Sr] of the culture seawater were maintained by additions of 0.6M $Na_2CO_3$ and a mixture of 0.58M $CaCl_2$ + 0.02M $SrCl_2$ by 200 µl volume solenoid diaphragm pumps, evenly spaced over a 24 hour period, controlled by a custom-written MATLAB® dosing control program (Cole et al., 2016). Seawater samples were collected weekly during the experimental period and analysed by quadrupole ICP-MS (Thermo Scientific X Series) for Mg, Ba and Ca. Samples were diluted 1000-fold in 5% $HNO_3$ (with 5 ppb In as an internal standard) and calibrated against matrix-matched synthetic standards prepared from 1000 µg $ml^{-1}$ single-element stock solutions (Inorganic Ventures) in 5% $HNO_3$. Replicate analyses of IAPSO standard seawater yielded Mg/Ca and Ba/Ca precision of 0.094 mol $mol^{-1}$ and 1.3 µmol $mol^{-1}$ respectively.

### 2.2 Secondary Ion Mass Spectrometry (SIMS)

The skeletons were sawn perpendicular to the growth surface of the coral skeleton to expose the centre of each colony and a section was cut along the axis of maximum linear extension. Sections were fixed in epoxy resin (Epofix, Struers Ltd.) in 2.5 cm circular moulds, under vacuum. The sections were polished using silicon carbide papers (up to 4000 grade, lubricated with water) and polishing alumina (0.05 µm, suspended in water) to produce a cross-section across the outermost surface of the skeleton, including the stain line. Sections were gold coated and analysed using a Cameca imf-4f ion microprobe in the School of Geosciences at the University of Edinburgh. Instrument conditions were $^{16}O^-$ beam, accelerated at 10.8 keV. The secondary ion extraction field was 4.5 KeV so the net impact energy of the primary ion beam was 15.1 KeV. Energy offset = 75 eV, energy window = 40 eV, imaged field = 25 µm, field aperture 1

and contrast aperture 2. We used a primary beam current of ~8 nA, a beam diameter of ~25 µm and a pre-analysis sputter of 1 minute to remove surface contamination. Each analysis is the sum of ten cycles and, for each cycle, we collected secondary singly-charged cations at masses $^{26}Mg$ (3 s), $^{44}Ca$ (2 s) and $^{138}Ba$ (15 s). Count rates were typically ~2000, ~230000 and ~80 counts per second (cps) respectively. The total time per analysis (including other isotopes not reported here) was 8 min and during this time the primary beam sputtered the sample to a depth of 2-3 µm (Allison et al., 2013). We estimate no significant isobaric interference for any of the isotopes studied (Allison 1996). Relative ion yields (RIY) for Mg/Ca and Ba/Ca were calculated from multiple (n = 9-27) daily analyses of a deep sea coral aragonite standard, NAHaxby2. We estimate the Mg/Ca composition of this standard as ≈ 65 mmol $mol^{-1}$ and Ba/Ca ≈ 0.0155 mmol $mol^{-1}$ by comparing SIMS analyses of this and another coral also analysed by bulk methods (Allison et al., 2007). The standard deviation of multiple standard analyses was typically 1.4% and 2.0% for Mg/Ca and Ba/Ca respectively. For analysis of each coral, multiple analyses (n = 12-41) were evenly spaced across the skeleton deposited during the experimental period (between the stain line and the outermost edge of the skeleton) across 2-3 different corallites of each colony. High Ba/Ca values have been reported in some SIMS analyses on centres of calcification in the most recently deposited sections of Porites spp. skeletons (Allison and Finch 2007) indicating that sodium hypochlorite cleaning may not remove all organic contamination in these areas. These features, which appear as dark hollows on the section surface in reflected light (Allison and Finch 2009) were avoided in this study. Analyses were also spatially removed, typically by several mm, from the skeleton deposited before import of the corals into the laboratory. Two replicate colonies of the *P. murrayensis* genotype were cultured and analysed in 400 and 750 µatm seawater $pCO_2$. We calculated the mean and standard deviation of analyses in each coral sample.

## 3. Results

### 3.1 Seawater chemistry

All seawater and skeletal data are summarised in Supplementary data table 1. Reservoir seawater Mg/Ca was comparable to natural seawater (Culkin and Cox, 1966) but reservoir Ba/Ca was higher than that reported from coral reef sites (~3 to 7-10 µmol $mol^{-1}$, Walther et al., 2013; LaVigne et al. 2016). Reservoir seawater [Ca] and Mg/Ca were stable (within analytical error) over the 5 week experimental period (Table 1) and variations between reservoirs are not significant (2 tailed t test, $p>0.05$). In contrast, seawater Ba/Ca varied significantly between all reservoirs (2 tailed t test, $p<0.05$, Table 1) and is negatively correlated with seawater $pCO_2$. Coral calcification and additions of the $Na_2CO_3$ and $CaCl_2$+$SrCl_2$ dosing solutions used to replace the ions consumed in calcification were highest at low seawater $pCO_2$. It is likely that the Ba/Ca of the $CaCl_2$+$SrCl_2$ dosing solution was higher than that of the reservoir seawater. Larger additions to the 180 µatm $pCO_2$ treatment during the coral acclimation period (to replace the ions used in calcification) generated a higher seawater Ba/Ca in this treatment. Similarly, larger additions over the 5 week experimental period resulted in a discernible increase in seawater Ba/Ca during this time i.e. seawater Ba/Ca increased over the experimental period by 17% at 180 µatm $pCO_2$ and by several % at 400 µatm $pCO_2$ (Figure 1a).

### 3.2 Coral skeletal Ba/Ca and Mg/Ca

Coral skeletal Ba/Ca and Mg/Ca are illustrated for each coral in Figure 2a and b. We observe no significant differences (2 tailed t test, $p<0.05$) in skeletal Ba/Ca between the duplicate *P. murrayensis* genotype colonies in 400 and 750 µatm seawater $pCO_2$ or in Mg/Ca at 750 µatm (Figure 2). However skeletal Mg/Ca varies significantly ($p = 0.0013$) between the duplicates cultured at 400 µatm and is ~30% higher in one individual.

We observe close agreement between trends of increasing seawater and skeletal Ba/Ca over the 5 week experimental period in both analysed corallites of the *P. lutea* 1 coral in 180 µatm seawater $pCO_2$ (Figure 1b) but similar trends are obvious in only one of 2 corallites analysed in the same coral genotype at 400 µatm seawater $pCO_2$. The increase in seawater Ba/Ca at 400 µatm is smaller than at 180 µatm (Figure 1a) and errors in seawater and skeletal analyses make detection of trends difficult in this treatment. We do not plot trends in 750 µatm seawater $pCO_2$ as variations in seawater Ba/Ca in this treatment are very small (Figure 1a). To remove the effect of variations in seawater Ba/Ca between seawater $pCO_2$ treatments we present coral skeletal Ba data as Ba/Ca seawater:aragonite partition coefficients (Figure 2c), hereafter abbreviated to $K_D$ Ba/Ca ($K_D$ Ba/Ca = skeletal Ba/Ca/seawater Ba/Ca). We also present skeletal Mg data as $K_D$ Mg/Ca (Figure 2d).

We compare skeletal Ba/Ca and Mg/Ca between different coral genotypes cultured in the same seawater $pCO_2$ by one way ANOVA (Table 2). All SIMS analyses for each coral genotype are combined for each seawater $pCO_2$ treatment i.e. data from the 2 replicate *P. murrayensis* colonies cultured at 400 and 750 µatm are combined for this analysis. Significant variations in skeletal Ba/Ca occur between individuals of different genotypes cultured at the same conditions (Table 2) Skeletal Ba/Ca for *P. lutea* 1 are significantly higher than for *P. lutea* 2 or the *P. murrayensis*, irrespective of seawater $pCO_2$ (Table 2). Skeletal Ba/Ca is significantly higher in *P. lutea* 2 compared to the *P. murrayensis* at 750 µatm. We observe significant differences in skeletal Mg/Ca between colonies but these are not systematic e.g. skeletal Mg/Ca in *P. lutea* 1 is significantly higher than in both *P. lutea* 2 and *P. murrayensis* at 180 µatm but is significantly lower than *P. lutea* 2 and is not significantly different from *P. murrayensis* at 750 µatm (Table 2, Figure 2b).

Comparing coral Ba/Ca between seawater $pCO_2$ treatments is more difficult due to the temporal trends in seawater Ba/Ca over the experimental period in the 180 and 400 µatm seawater $pCO_2$ treatments. We normalise skeletal Ba/Ca of each SIMS analysis to the mean experimental period seawater Ba/Ca in each treatment and compare the resulting $K_D$ Ba/Ca by one way ANOVA (Table 3). In so doing we are assuming that calcification of each colony is approximately constant throughout the experimental period. Seawater Ba/Ca and skeletal Ba/Ca show similar proportional increases over the experimental period suggesting that this is a reasonable assumption (Figure 1b). To ensure that variations in seawater Ba/Ca did not affect this statistical interpretation we repeated this normalisation using both the highest and lowest seawater Ba/Ca observed over the experimental period. $K_D$ Ba/Ca is significantly lower at 180 µatm than at 750 µatm in *P. lutea* 2 regardless of normalisation procedure (Table 3, Figure 2c). $K_D$ Ba/Ca is significantly lower at 180 µatm than at 400 µatm in the *P. murrayensis* (Table 3) when SIMS data are normalised to the mean seawater Ba/Ca to calculate $K_D$ Ba/Ca but these corals are not significantly different when SIMS data are normalised to high seawater Ba/Ca. No other significant differences were observed in $K_D$ Ba/Ca between $pCO_2$ treatments, regardless of the normalisation procedure.

We compared $K_D$ Mg/Ca between individuals of the same genotype cultured under different seawater $pCO_2$ using one way ANOVA (Table 3). Variations in $K_D$ Mg/Ca between seawater $pCO_2$ treatments are not consistent e.g. $K_D$ Mg/Ca is significantly higher at 180 µatm than at 750 µatm in *P. lutea* 1 but the relationship is reversed in *P. lutea* 2 (Table 3, Figure 2d).

### 3.2.2. Relationships with physiological processes

Calcification was significantly reduced at 750 µatm compared to 180 µatm seawater $pCO_2$ in the *P. lutea* 2 and *P. murrayensis* genotypes (Cole et al., 2018) but did not vary significantly as a function of seawater $pCO_2$ in *P. lutea 1*. We plotted $K_D$ Ba/Ca and $K_D$ Mg/Ca versus calcification, respiration and net and gross photosynthesis for each colony as a function of coral genotype (Figure 3).

In so doing we are matching the chemistry of the skeleton deposited in the 5 week experimental period with physiological measurements made over the same interval (Cole et al., 2018). Some of the correlation coefficients between physiological rates and $K_D$ Ba/Ca and $K_D$ Mg/Ca are high (Table 4) but in only one case is the correlation significant, reflecting the small number of samples (n = 3-5). $K_D$ Mg/Ca is significantly negatively correlated with calcification rate in *P. lutea* 2. We do not observe consistent relationships between physiological rates and $K_D$ Ba/Ca and $K_D$ Mg/Ca.

### 3.2.2. Relationships between elements

To explore the interactions of different skeletal elements we plotted relationships between mean $K_D$ Ba/Ca, $K_D$ Mg/Ca and $K_D$ Sr/Ca (from Cole et al., 2016) for each individual coral. We plotted regressions, grouping the corals by genotype, (Figure 4) and calculated correlation coefficients (Table 5). None of these correlations is significant ($p \leq 0.05$) due to the small numbers (n = 3-5) in each regression group. $K_D$ Mg/Ca and $K_D$ Sr/Ca are negatively correlated in both genotypes of *P. lutea* but in only one case is the correlation strong (*P. lutea* 1, $r^2 = 0.85$). We do not observe systematic behaviour in other elements between genotypes.

## 4. Discussion

### 4.1 Coral $K_D$ Ba/Ca

We observe large variations in $K_D$ Ba/Ca, from ~0.5 to 1.5, between different coral genotypes grown in the same tanks (Figure 2). Our higher estimates of $K_D$ Ba/Ca are in reasonable agreement with previous reports for *Porites* spp. in the field ($K_D$ = 1.2, LaVigne et al., 2016) and for aragonites synthetically precipitated at 25°C from seawater ($K_D$ = 2.1, Gaetani and Cohen, 2006) and from $Ca^{2+}$-$Mg^{2+}$-$Cl^-$ solutions (ionic strength ~0.1M, $K_D$ = 1.5, Dietzel et al., 2004). Higher and lower $K_D$ Ba/Ca ($K_D$ = 3.8, Pretet et al., 2016; $K_D$ = 0.9, Gonneea et al., 2017) are occasionally observed in cultured corals but extreme values are unusual. In our study all corals appeared healthy throughout the experiment and physiological rates (Figure 3) are comparable to measurements of calcification (Allison et al., 1996) and photosynthesis and respiration (Hennige et al., 2010) in field specimens of massive *Porites* spp. Seawater Ba/Ca in our aquaria are high compared to natural waters and we cannot rule out the possibility that the relationship between seawater and skeletal Ba/Ca may be non-linear in some coral genotypes. However a linear relationship has been observed between seawater Ba/Ca and skeletal Ba/Ca in juvenile *Favia fragum* colonies cultured over a range of seawater Ba/Ca which extends to values similar to those used in our study.

#### 4.1.1 Coral genotype and $K_D$ Ba/Ca

$K_D$ Ba/Ca for *P. lutea* 1 are x 2-3 higher than for *P. lutea* 2 or the *P. murrayensis*, irrespective of seawater $pCO_2$ (Figure 2). LaVigne et al. (2016) observed good agreement in skeletal Ba/Ca of multiple *P. lobata* colonies from the same reef site and our finding that massive adult *Porites* spp. corals of the same species incorporate widely varying skeletal Ba/Ca under constant conditions is, to our knowledge, unique. Large variations in $K_D$ Ba/Ca (up to x2) have also been reported between individual juvenile *Favia fragum* colonies settled and grown in aquaria under the same seawater temperatures and seawater Ba/Ca (Gonneea et al. 2017). However calcite is present in the basal plates of newly settled coral recruits (Gilis et al., 2014) and $K_D$ Ba/Ca variations between juvenile corals may reflect varying mixtures of calcite and aragonite which exhibit different Ba/Ca partitioning. The mineral phase of adult corals is solely aragonitic (Gilis et al., 2014) and variations in mineralogy cannot explain the $K_D$ Ba/Ca variations observed here.

Variations in skeletal Ba/Ca may reflect changes in the composition of the calcification fluid used for skeletal construction. The aragonite skeleton precipitates from a calcification fluid enclosed in a space between the basal coral tissue and the underlying skeleton (Clode and Marshall, 2002). The calcification fluid probably derives from seawater transported paracellularly (between cells) to the calcification site (Tambutte et al., 2012). The fluid composition is modified by the addition or removal of solutes during fluid transport or whilst at the site e.g. $Ca^{2+}$ is transported across cell walls via L-type Ca channels (Marshall 1996; Tambutte et al., 1996; Zoccola et al., 1999) and the enzyme Ca-ATPase (Ip et al., 1991; Marshall, 1996).

Several mechanisms may affect fluid and/or skeletal Ba/Ca. Increases in transcellular $Ca^{2+}$ transport probably reduce calcification fluid Ba/Ca and thereby skeletal Ba/Ca. Ca channels likely increase fluid [$Ca^{2+}$] while Ca-ATPase increases both the [$Ca^{2+}$] and pH of the calcification fluid (Al Horani et al., 2003). Both of these increase the aragonite saturation state of the calcification fluid as the pH increase serves to concentrate dissolved inorganic carbon at the calcification site (Erez 1978; McConnaughey 2003). Coral calcification rates are positively correlated with the saturation states of the calcification fluid (Allison et al., 2014) and seawater (Gattuso et al., 1998) so if this hypothesis is correct then we expect low skeletal Ba/Ca (reflecting high transcellular $Ca^{2+}$ transport) to occur at rapid calcification rates. The composition of the calcification fluid may also be affected by the amount of aragonite precipitated from it if the fluid acts as a semi-isolated reservoir (Rayleigh fractionation, Elderfield et al., 1996) and if $Ba^{2+}$ competes with $Ca^{2+}$ for inclusion in the aragonite lattice. The $K_D$ Ba/Ca of inorganic aragonite is >1 (Dietzel et al., 2004; Gaetani and Cohen, 2006) so the Ba/Ca of the fluid remaining in the reservoir, and of the aragonite precipitated from it, decreases as precipitation proceeds. Precipitation of a large proportion of the fluid reservoir results in low skeletal Ba/Ca. Finally, the growth entrapment model suggests that disequilibrium partitioning of metal/Ca may occur in carbonates at rapid precipitation rates (Watson 1994; Gabitov et al., 2014). As the $K_D$ Ba/Ca of inorganic aragonite is >1, then this model predicts a low aragonite Ba/Ca at fast precipitation rates.

We do not observe systematic variations in the calcification rates of the different coral genotypes which would support these explanations. The fastest growing individuals of each coral genotype (those cultured at 180 µatm, Cole et al., 2018) attained broadly comparable calcification rates (Figure 3) yet these corals display widely varying $K_D$ Ba/Ca.

Predicting the impact of Rayleigh fractionation and the growth entrapment model on skeletal Ba/Ca in our dataset assumes that $Ba^{2+}$ substitutes in place of $Ca^{2+}$ in the aragonite lattice. However the Ba structural state in coral aragonite is unknown (Finch et al., 2010). Coral skeletons are composite materials and some trace/minor element ions are substituted into the aragonite mineral e.g. Sr (Finch and Allison, 2003) while others may be hosted by an alternative phase e.g. Mg (Finch and Allison, 2008, Farges et al., 2009) and S (Cuif and Dauphin, 2005). If Ba is predominantly associated with a non-aragonite phase then variations in the proportion or, if organic, the composition of this phase, may affect skeletal Ba/Ca incorporation.

### 4.1.2 Seawater $pCO_2$ and $K_D$ Ba/Ca

$K_D$ Ba/Ca are significantly higher at 750 µatm than at 180 µatm in 1 of the 3 coral genotypes (*P. lutea* 2) but in the other 2 coral genotypes no significant effect of seawater $pCO_2$ can be determined. Seawater $pCO_2$ may affect skeletal Ba/Ca incorporation if seawater $pCO_2$ impacts the calcification fluid Ba/Ca. At high seawater $pCO_2$, corals increase the pH (and decrease the [$H^+$]) of the calcification fluid above that of seawater more than in their lower seawater $pCO_2$ counterparts (Venn et al., 2012). If this pH increase reflects proton extrusion by Ca-ATPase (e.g. Al Horani et al., 2003) then it is reasonable to assume that corals at high seawater $pCO_2$ pump more $Ca^{2+}$ into the calcification site. This could dilute calcification fluid Ba/Ca. This explanation does not fit our data where $K_D$ Ba/Ca are higher at high seawater $pCO_2$.

Calcification rates were reduced at 750 µatm compared to 180 µatm in both *P. lutea* 2 and *P. murrayensis* (Cole et al., 2018). Skeletal Ba/Ca is negatively correlated with calcification rate in all coral genotypes (Figure 3) but none of these relationships is significant due to the small sample numbers (Table 4). We do not observe significant variations in the calcification rates of *P. lutea* 1 between $pCO_2$ treatments and variations in $K_D$ Ba/Ca between these corals are small. An inverse correlation between calcification rate and $K_D$ Ba/Ca could be explained by Rayleigh fractionation (precipitation of a large proportion of the fluid reservoir will generate low aragonite Ba/Ca) or the growth entrapment model (rapid precipitation rates generate low aragonite Ba/Ca). However Rayleigh fractionation predicts positive correlations between observed $K_D$ Ba/Ca and $K_D$ Sr/Ca as the $K_D$ Ba/Ca and $K_D$ Sr/Ca of inorganic aragonite are both >1 (Dietzel et al., 2004; Gaetani and Cohen, 2006). However correlations between $K_D$ Ba/Ca and $K_D$ Sr/Ca (from Cole et al., 2016) for each coral, grouped by genotype, are insignificant and usually weak (Table 5). Furthermore our observation, that $K_D$ Ba/Ca is negatively correlated with calcification rate (Table 4, Figure 3), contrasts with observations of *Porites* spp. field colonies in which skeletal Ba/Ca was significantly higher (by ~20%) in a slow-growing specimen compared to an adjacent fast growing individual (Allison and Finch 2007). How seawater $pCO_2$ affects skeletal Ba/Ca is unknown but changes in seawater $pCO_2$ likely affect multiple coral processes which may influence Ba/Ca incorporation.

### 4.2 Coral $K_D$ Mg/Ca

We observed large variations in skeletal Mg/Ca between duplicate colonies of the same genotype cultured at 400 µatm. XAFS indicates that coral skeletal Mg is not predominantly substituted for Ca in aragonite but is included in an alternative phase (Finch et al., 2008, Farges et al., 2009; Yoshimura et al., 2015) e.g. an organic material or amorphous calcium carbonate. $Mg^{2+}$ affects $CaCO_3$ polymorph and morphology (Falini et al., 2013) and is implicated in the control of coral biomineralisation (Sancho-Tomas et al., 2014). $Mg^{2+}$ can facilitate (Falini et al., 2009, Tao et al., 2009) or inhibit (Addadi et al., 2003) $CaCO_3$ precipitation possibly by interacting with different organic molecules present at the calcification site (Falini et al., 2013). Variations in skeletal Mg/Ca between duplicate colonies may reflect differences in calcification fluid Mg/Ca or changes in the proportions or compositions of the Mg-bearing phase. These variations are large and may overwrite any environmental effect on Mg incorporation (Mitsuguchi et al., 1996). We do not observe consistent relationships between $K_D$ Mg/Ca and seawater $pCO_2$. Similarly we do not observe systematic relationships between coral physiological processes (calcification, photosynthesis and respiration, Figure 3) and skeletal Mg/Ca, or between $K_D$ Mg/Ca and $K_D$ Ba/Ca or $K_D$ Sr/Ca (Figure 4).

### 4.3 Implications for reconstruction of environmental and palaeoenvironmental records

Coral aragonite Ba/Ca correlates well with seawater Ba/Ca (LaVigne et al., 2016) and coral skeletal records has been used to infer oceanic upwelling (Lea et al. 1989) and/or local rainfall and freshwater runoff (Sinclair and McCulloch, 1994). While $K_D$ Ba/Ca is known to vary significantly between coral genera (LaVigne et al., 2016; Pretet et al., 2016), our study also demonstrates that $K_D$ Ba/Ca can vary significantly (by x2-3) between adult specimens of the same genera and even between individuals of the same coral species. Fossilised massive Porites spp. corals are not usually identified to species level as the corallite morphology at the growing coral surface is rarely preserved. The consequences of these variations will be limited if skeletal Ba/Ca is used to infer changes in ocean circulation or freshwater discharges within a single coral record (Sinclair and McCulloch, 1994). However if multiple coral records are compared e.g. to infer the significance of freshwater discharges between sites (Prouty et al., 2010) or to estimate changes in ocean circulation over geological time (Montaggioni et al., 2006), then the implications of variations in $K_D$ Ba/Ca are significant. Seawater Ba/Ca can vary by ~ x2 in regions affected by upwelling and

terrestrial run-off (LaVigne et al., 2016). Genotype specific variations in $K_D$ Ba/Ca can be of a similar or greater magnitude so could overwhelm any skeletal signature of seawater Ba/Ca in inter-coral comparisons.

Our data also suggest that seawater $pCO_2$ can affect skeletal Ba/Ca in some *Porites* sp. genotypes. $K_D$ Ba/Ca is significantly lower at 180 µatm than at 750 µatm (by 33%) in 1 coral genotype. $K_D$ Ba/Ca is lower at 180 µatm than at 400 µatm (by 13-16%) in 2 corals but these effects are not significant. Fossil coral specimens deposited at lower seawater $pCO_2$, may underestimate past seawater Ba/Ca and thereby underestimate ocean upwelling or freshwater inputs when compared with more modern specimens however any affect will be very subtle as the magnitude of the seawater $pCO_2$ effect is small in comparison with the $K_D$ Ba/Ca variation observed between genotypes.

## 5. Conclusions

$K_D$ Ba/Ca do not vary significantly between duplicate colonies of the same massive *Porites* sp. coral genotype but can vary significantly between adult specimens of the same genera and even between individuals of the same coral species cultured under the same environmental conditions. This has implications for the use of coral skeletons as indicators of seawater Ba/Ca and therefore of ocean upwelling or freshwater runoff. Genotype variations are large (up to x2-3) and could overwrite any environmental signature or imply significant variations in seawater Ba/Ca.

Variations in $K_D$ Ba/Ca do not correlate with coral calcification, photosynthesis or respiration rates or with skeletal $K_D$ Mg/Ca or $K_D$ Sr/Ca and their origin is unresolved. $K_D$ Ba/Ca is significantly higher at 750 µatm seawater $pCO_2$ than at 180 µatm in 1 of the 3 coral genotypes suggesting that seawater $pCO_2$ (known to vary over geological time) could affect Ba/Ca in some coral skeletons. .

**Acknowledgments**

This work was supported by the UK Natural Environment Research Council (award NE/I022973/1) to AAF and NA. NERC Scientific Services provided access to the ion microprobe, and we are indebted to Richard Hinton for his assistance with the analyses. Seawater Ba/Ca and Mg/Ca analyses were carried out by Matt Cooper (University of Southampton). We thank Dave Steven, Mark Robertson, Casey Perry, Mike Scaboo and Andy Mackie for their assistance with the culture system build.

**References**

Addadi, L., Raz, S., Weiner, S., 2003. Taking advantages of disorder: amorphous calcium carbonate and its role in biomineralization. Adv. Mater. 15, 959–970.

Al-Horani, F.A., Al-Moghrabi, S.M., de Beer, D., 2003. The mechanism of calcification and its relation to photosynthesis and respiration in the scleractinian coral *Galaxea fascicularis*. Mar. Biol. 142, 419-426.

Allison N., 1996. Quantitative determinations of trace and minor elements in coral aragonite by ion microprobe analysis, with preliminary results from Phuket, South Thailand. Geochim. Cosmochim. Acta 60, 3457-3470.

Allison, N., Chambers, D., Finch, A.A., E.I.M.F., 2013. SIMS sputtering rates in biogenic aragonite: implications for culture calibration studies for palaeoenvironmental reconstruction. Surface Interface Anal. 45, 1389-1394.

Allison, N., Cohen, I., Finch, A.A., Erez, J., Tudhope, A.W., 2014. Corals concentrate dissolved inorganic carbon to facilitate calcification. Nature Communications *5***,** 5741 doi: 10.1038/ncomms6741.

Allison, N., Finch, A.A., 2007. High temporal resolution Mg/Ca and Ba/Ca records in modern *Porites lobata* corals. Geochem. Geophys. Geosyst. 8, Q05001 doi 10.1029/2006GC001477.

Allison, N., Finch, A.A., Webster, J.M., Clague, D.A., 2007. Palaeoenvironmental records from fossil corals: the effects of submarine diagenesis on temperature and climate estimates. Geochim. Cosmochim. Acta. 71, 4693-4703.

Allison, N., Tudhope, A.W., Fallick, A.E., 1996. Factors influencing the stable carbon and oxygen isotopic composition of *Porites lutea* coral skeletons from Phuket, South Thailand. Coral Reefs, 15, 43-57.

Castillo, K.D., Ries, J.B., Bruno, J.F., Westfield, I.T., 2014. The reef-building coral *Siderastrea siderea* exhibits parabolic responses to ocean acidification and warming. Proceedings of the Royal

Society of London B: Biological Sciences, 281, doi: 10.1098/rspb.2014.1856.

Chan, L.H., Drummond, D., Edmond, J.M., Grant, B., 1977. On the barium data from the Atlantic GEOSECS expedition. Deep-Sea Research 24, 613-649.

Clode, P.L., Marshall, A.T., 2002. Low temperature FESEM of the calcifying interface of a scleractinian coral. Tissue and Cell 34, 187-198.

Cole, C., Finch, A.A., Hintz, C., Hintz, K., Allison, N., 2016. Understanding cold bias: variable response of skeletal Sr/Ca to seawater $pCO_2$ in acclimated massive *Porites* corals. Scientific Reports 6, 26888; doi: 10.1038/srep26888.

Cole, C., Finch, A.A., Hintz, C., Hintz, K., Allison, N., 2018. Effects of seawater $pCO_2$ and temperature on calcification and productivity in the coral genus *Porites* spp.: an exploration of potential interaction mechanisms. Coral Reefs, doi.org/10.1007/s00338-018-1672-3.

Cuif, J.-P., Dauphin, Y., 2005. The environment recording unit in coral skeletons – a synthesis of structural and chemical evidences for a biochemically driven, stepping-growth process in fibres. Biogeosciences, 2, 61-73.

Culkin, F., Cox, R.A., 1966. Sodium, potassium, magnesium, calcium and strontium in sea water. Deep-Sea Res., 13: 789-804.

de Villiers, S., Shen, G.T., Nelson, B.K., 1994. The Sr/Ca-temperature relationship in coralline

aragonite: influence of variability in (Sr/Ca)seawater and skeletal growth parameters. Geochim. Cosmochim. Acta, *58*, 197-208.

de Villiers, S., Nelson, B.K., Chivas, A.R., 1995. Biological controls on coral Sr/Ca and d18O reconstructions of sea surface temperatures. Science, 269, 1247-9.

Dietzel, M., Gussone, N., Eisenhauer, A., 2004. Co-precipitation of Sr2+ and Ba2+ with aragonite by membrane diffusion of $CO_2$ between 10 and 50°C. Chem. Geol. 203, 139-151.

Edmunds, P.J., Burgess, S.C., 2016. Size-dependent physiological responses of the branching coral *Pocillopora verrucosa* to elevated temperature and $pCO_2$. Journal of Experimental Biology, 291, 3896-3906.

Elderfield, H., Bertram, C.J., Erez, J. 1996. Biomineralization model for the incorporation of trace elements into foraminiferal calcium carbonate. Earth Planet. Sci. Lett. 142, 409-423.

Erez, J., 1978. Vital effect on the stable-isotope composition seen in foraminifera and coral skeletons. Nature 273, 199-202.

Falini, G., Fermani, S., Tosi, G., Dinelli, E., 2009. Calcium carbonate morphology and structure in the presence of seawater ions and humic acids. Cryst. Growth Des., 9, 2065–2072, doi: 10.1021/cg8002959.

Falini, G., Reggi, M., Fermani, S., Sparla, F., Goffredo, S., Dubinsky, Z., Cuif, J.-P., 2013. Control of aragonite deposition in colonial corals by intra-skeletal macromolecules. J. Struct. Biol. 183, 226-238.

Farges, F., Meibom, A., Flank, A.M., Lagarde, P., Janousch, M., Stolarski, J., 2009. Speciation of Mg in biogenic calcium carbonates. Journal of Physics: Conference Series 190**,** doi:10.1088/1742-6596/190/1/012175.

Finch, A.A., Allison, N., 2003. Strontium in coral aragonite: 2. Sr co-ordination and the long-term stability of environmental records. Geochim. Cosmochim. Acta *67*, 4519-4527.

Finch, A.A., Allison, N., 2008. Mg structural state in coral aragonite and implications for the paleoenvironmental proxy. Geophysical Research Letters 35, L08704, doi 10.1029/2008GL033543.

Finch, A.A., Allison, N., Steaggles, H., Wood, C.V., Mosselmans, J.F.W., 2010. Ba XAFS of Ba-rich standard minerals and the potential for determining Ba structural state in calcium carbonate. Chem. Geol. 270, 179-185.

Gabitov, R.I., Sadekov, A., Leinweber, A., 2014. Crystal growth rate effect on Mg/Ca and Sr/Ca partitioning between calcite and fluid: an in situ approach. Chem. Geol. 367 70-82 doi: 10.1016/j.chemgeo.2013.12.019.

Gaetani, G.A., Cohen, A.L., 2006. Element partitioning during precipitation of aragonite from seawater: a framework for understanding paleoproxies. Geochim. Cosmochim. Acta, 70, 4617-4634.

Gattuso, J.-P., Frankignoulle, M., Bourge, I., Romaine, S., Buddemeier, R.W., 1998. Effect of calcium carbonate saturation of seawater on coral calcification. Global and Planetary Change 18, 37-46 doi.org/10.1016/S0921-8181(98)00035-6.

Gattuso, J.-P., Lavigne, H., 2009. Technical Note: Approaches and software tools to investigate the impact of ocean acidification. *Biogeosciences, 6*, 2121–2133.

Gilis, M., Meibom, A., Doart-Coulon, I., Grauby, O., Stolarski, J., Beronnet,A., 2014. Biomineralization in newly settled recruits of the scleractinian coral *Pocillopora damicornis,* J. Morphology, 275, doi: 10.1002/jmor.20307.

Gonneea, M.E., Cohen, A.L., DeCarlo, T.M., Charette, M.A., 2017. Relationship between water and aragonite barium concentrations in aquaria reared juvenile corals. Geochim. Cosmochim. Acta. 209, 123-134.

Hennige, S.J., Smith, D.J., Walsh, S.J., McGinley, M.P., Warner, M.E., Suggett, D.J., 2010. Acclimation and adaptation of scleractinian coral communities along environmental gradients within an Indonesian reef system, J. Exp. Mar. Bio. Ecol., 391, 153-152.

Holcomb, M., DeCarlo, T.M., Gaetani, G.A., McCulloch, M., 2016. Factors affecting B/Ca ratios in synthetic aragonite. Chem. Geol. 437, 67-76.

Ip, Y.K., Lim, A.L.L., Lim, R.W.L., 1991. Some properties of calcium-activated adenosine-triphosphatase from the hermatypic coral *Galaxea fascicularis*. Mar. Biol. 111: 191-197.

IPCC Climate Change 2013, 2013. The Physical Science Basis. (eds T.F. Stocker and D.Qin) Cambridge Univ. Press, Cambridge, U.K.

LaVigne, M., Grottoli, A.G., Palardy, J.E., Sherrell, R.M., 2016. Multi-colony calibrations of coral Ba/Ca with a contemporaneous in situ seawater barium record. Geochim. Cosmochim. Acta 179, 203-216.

Lea, D.W., Shen, G.T., Boyle, E.A., 1989. Coralline barium records temporal variability in equatorial Pacific upwelling, Nature, 340, 373 – 376, doi:10.1038/340373a0.

Marshall, A.T., 1996. Calcification in hermatypic and ahermatypic corals, Science 271, 637-639.

McConnaughey, T.A., 2003. Sub-equilibrium oxygen-18 and carbon-13 levels in biological carbonates: carbonate and kinetic models. Coral Reefs 22, 316-327.

Mitsuguchi, T., Matsumoto, E., Abe, O., Uchida, T., Isdale, P.J., 1996. Mg/Ca thermometry in coral skeletons, Science, 274, 961-3.

Montaggioni, L.F., Le Cornec, F., Corrège, T., Cabioch, G., 2006. Coral barium/calcium record of mid-Holocene upwelling activity in New Caledonia, South-West Pacific. Palaeogeography Palaeoclimatology Palaeoecology 237, 436-455.

Petit, J.R., Jouzel, J., Raynaud, D., Barkov, N.I., Barnola, J.-M., Basile, I., Stievenard, M., 1999. Climate and atmospheric history of the past 420 ky from the Vostok ice core. Antarctica. Nature 399, 429-436.

Pretet, C.E., Zuilen, K.V., Nagler, T.F., Reynaud, S., Bottcher, M.E., Samankassou, E., 2015. Constraints on barium isotope fractionation during aragonite precipitation by corals. The Depositional Record 1, 118–129.

Prouty, N.G., Field, M.E., Stock, J.D., Jupiter, S.D., McCulloch, M., 2010. Coral Ba/Ca records of sediment input to the fringing reef of the southshore of Moloka'i, Hawai'i over the last several decades. Mar. Pollut. Bull. 60, 1822-35.

Sancho-Tomás M., Fermani, S., Goffredo, S., Dubinsky, Z., García-Ruiz, J.M., Gómez-Morales, J., Falini, G., 2014. Exploring coral biomineralization in gelling environments by means of a counter diffusion system. CrystEngComm. 16, 1257 – 1267.

Sinclair, D.J., McCulloch, M.T., 2004. Corals record low mobile barium concentrations in the Burdekin River during the 1974 flood: evidence for limited Ba supply to rivers? Palaeogeography Palaeoclimatology Palaeoecology, *214*, 155-174.

Spencer Davies P., 1991. Effect of daylight variations on the energy budgets of shallow-water corals. Mar, Biol. 108, 137-144.

Tambutte, E., Allemand, D., Mueller, E., Jaubert, J., 1996. A compartmental approach to the mechanism of calcification in hermatypic corals. J. Exp.Biol, 199**,** 1029-1041.

Tambutte, E., Tambutté, S., Segonds, N., Zoccola, D., Venn, A., Erez, J., Allemand, D., 2012. Calcein labelling and electrophysiology: insights on coral tissue permeability and calcification. Proc. Royal Soc. B 279, 19-27.

Tao, J., Zhou, D., Zhang, Z., Tang, R., 2009. Magnesium-aspartate-based crystallization switch inspired from shell molt of crustacean. Proc. Natl. Acad. Sci. U.S.A. 106, 22096–22101.

Venn, A.A., Tambutte, E., Holcomb, M., Tambutte, S., 2012. Impact of seawater acidification on pH at the tissue-skeleton interface and calcification in reef corals. Proc. Natl. Acad. Sci. 110, 1634-1639.

Vernon, J.E.N., 1993. Corals of Australia and the Indo-Pacific, University of Hawaii Press; 2nd edition.

Walther, B.D., Kingsford, M.J., McCulloch, M.T., 2013. Environmental records from Great Barrier Reef corals: inshore versus offshore drivers, PLOS One, 8, e77091, doi: 10.1371/journal.pone.0077091.

Watson, E., 1994. A conceptual model for near-surface kinetic controls on the trace-element and stable isotope composition of abiogenic calcite crystals. Geochim. Cosmochim. Acta 68, 1473-1488.

Yoshimura, T., Tamenon, Y., Takahashi, O., Nguyen, L.T., Hasegawa, H., Iwasaki, N., Kawahata, H., 2015. Mg coordination in biogenic carbonates constrained A. by theoretical and experimental XANES, Earth Planet. Sci. Lett., 421, 68-74.

Zoccola, D., Tambutte, E., Senegas-Balas, F., Michiels, J.F., Failla, J.P., Jaubert, J., Allemand, D., 1999. Cloning of a calcium channel alpha 1 subunit from the reef-building coral, *Stylophora pistillata*. Gene, 227, 157-167.

**Table 1.** Seawater compositions of different treatments. Values are means of 5 measurements over the experimental period ± standard deviation with coefficients of variation in parentheses.

| | 180 µatm | 400 µatm | 750 µatm |
|---|---|---|---|
| [Ca] (mmol $kg^{-1}$) | 9.78 ± 0.08 (0.8%) | 9.84 ± 0.10 (1.0%) | 9.86 ± 0.07 (0.7%) |
| Mg/Ca (mol $mol^{-1}$) | 5.92 ± 0.08 (1.4%) | 5.90 ± 0.08 (1.3%) | 5.88 ± 0.05 (0.8%) |
| Ba/Ca (µmol $mol^{-1}$) | 56.9 ± 4.6 (8.0%) | 36.7 ± 2.0 (5.3%) | 32.8 ± 0.9 (2.8%) |

**Table 2.** Summary of significant differences ($p \leq 0.05$) comparing skeletal Ba/Ca and Mg/Ca between individuals of different coral genotypes cultured in the same seawater $pCO_2$ treatments. Significant differences were identified by one way ANOVA followed by Tukey's pairwise comparisons. The data from the 2 replicate *P. murrayensis* colonies cultured at 400 and 750 µatm were combined for this analysis.

| ANOVA | | Seawater $pCO_2$ (µatm) | | |
|---|---|---|---|---|
| | | 180 | 400 | 750 |
| Skeletal Ba/Ca | *P. lutea* 1 and 2 | Pl1 > Pl2 | Pl1 > Pl2 | Pl1 > Pl2 |
| | *P. lutea* 1 and *P. murrayensis* | Pl1 > Pm | Pl1 > Pm | Pl1 > Pm |
| | *P. lutea* 2 and *P. murrayensis* | Pl2 = Pm | Pl2 = Pm | Pl2 > Pm |
| Skeletal Mg/Ca | *P. lutea* 1 and 2 | Pl1 > Pl2 | Pl1 = Pl2 | Pl1 < Pl2 |
| | *P. lutea* 1 and *P. murrayensis* | Pl1 > Pm | Pl1 = Pm | Pl1 = Pm |
| | *P. lutea* 2 and *P. murrayensis* | Pl2 = Pm | Pl2 = Pm | Pl2 > Pm |

**Table 3.** Summary of significant differences (p≤0.05) comparing $K_D$ Ba/Ca or $K_D$ Mg/Ca between individuals of the same coral genotype cultured in different seawater $pCO_2$ treatments.

| | | *P. lutea* 1 | *P. lutea* 2 | *P. murrayensis* |
|---|---|---|---|---|
| $K_D$ Ba/Ca | 180 and 400 µatm | 180 = 400 | 180 = 400 | 180 =< 400[a] |
| | 180 and 750 µatm | 180 = 750 | 180 < 750 | 180 = 750 |
| | 400 and 750 µatm | 400 = 750 | 400 = 750 | 400 = 750 |
| $K_D$ Mg/Ca | 180 and 400 µatm | 180 > 400 | 180 = 400 | 180 = 400 |
| | 180 and 750 µatm | 180 > 750 | 180 < 750 | 180 = 750 |
| | 400 and 750 µatm | 400 > 750 | 400 = 750 | 400 = 750 |

Significant differences were identified by one way ANOVA followed by Tukey's pairwise comparisons. The data from the 2 replicate genotype 3 colonies cultured at 400 and 750 µatm were combined for this analysis.

[a] $K_D$ Ba/Ca calculated using mean seawater Ba/Ca in corals cultured at 180 µatm were significantly different from those of corals cultured at 400 µatm but $K_D$ Ba/Ca calculated using the highest observed seawater Ba/Ca at 180 µatm were not significantly different from those of corals cultured at 400 µatm.

**Table 4.** Correlation coefficients ($r^2$) between $K_D$ Ba/Ca and $K_D$ Mg/Ca (this study) and physiological processes (Cole et al., 2018) in each coral genotype.

| | $K_D$ Ba/Ca | | | $K_D$ Mg/Ca | | |
|---|---|---|---|---|---|---|
| Genotype | Pl1 | Pl 2 | Pm | Pl1 | Pl 2 | Pm |
| Calcification | 0.45 | 0.92 | 0.38 | 0.52 | **1.00** | 0.052 |
| NP | 0.60 | 0.36 | 0.058 | 0.43 | 0.14 | 0.014 |
| GP | 0.56 | 0.42 | 0.078 | 0.47 | 0.18 | 0.009 |
| R | 0.31 | 0.70 | 0.18 | 0.72 | 0.001 | 0.000 |

Significant correlations (p<0.05) are highlighted in bold. Genotypes are abbreviated as in the legend to Figure 2.

**Table 5.** Correlations coefficients ($r^2$) between $K_D$ Ba/Ca, $K_D$ Mg/Ca (this study) and $K_D$ Sr/Ca (from Cole et al., 2016) for each coral colony as a function of genotype.

| | *P. lutea* 1 | *P. lutea* 2 | *P. murrayensis* |
|---|---|---|---|
| $K_D$ Ba/Ca and $K_D$ Sr/Ca | 0.12 | 0.12 | 0.33 |
| $K_D$ Ba/Ca and $K_D$ Mg/Ca | 0.0010 | 0.93 | 0.30 |
| $K_D$ Mg/Ca and $K_D$ Sr/Ca | 0.85 | 0.34 | 0.11 |

Figure 1. a) Changes in seawater Ba/Ca over the 5 week experimental period (error bar indicates standard deviation of repeat seawater analyses) and b) increases in skeletal Ba/Ca (over 2 transects of different corallites of *P. lutea* 1) and seawater Ba/Ca over the 5 week experimental period at 180 and 400 µatm seawater $pCO_2$. All points are shown as a proportion of the mean value. Skeletal Ba/Ca data have been scaled assuming that linear extension is constant over the 5 week period. The typical standard deviation of repeat analyses is indicated for all seawater points and as a floating error bar for skeletal Ba/Ca.

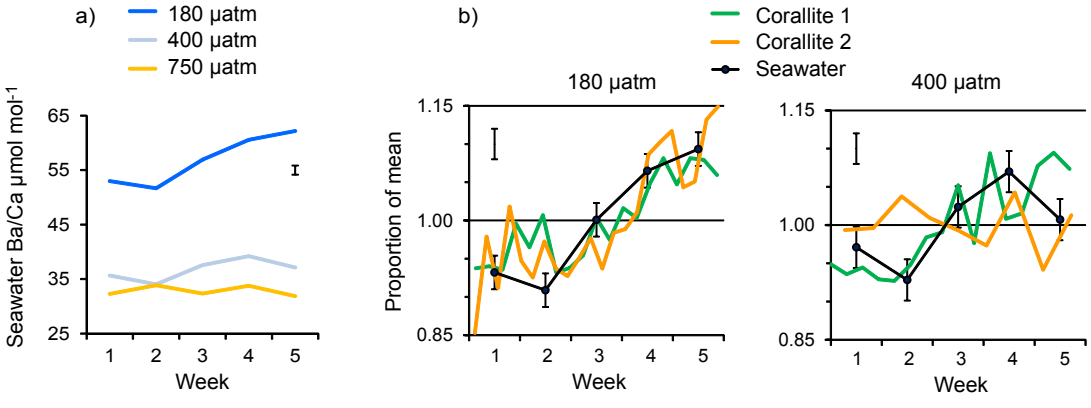


Figure 2. Skeletal concentrations of a) Ba/Ca (µmol $mol^{-1}$) and b) Mg/Ca (mmol $mol^{-1}$) and observed seawater:coral aragonite partition coefficients ($K_D$) of c) Ba/Ca and d) Mg/Ca. Error bars for skeletal concentrations indicate 95% confidence limits while error bars for $K_D$ compound 95% confidence limits for skeletal and seawater analyses. Skeletal concentrations are grouped per $pCO_2$ treatment while $K_D$ are grouped per coral genotype (Pl 1 = *P. lutea* 1, Pl 2 = *P. lutea* 2, Pm = *P. murrayensis*).

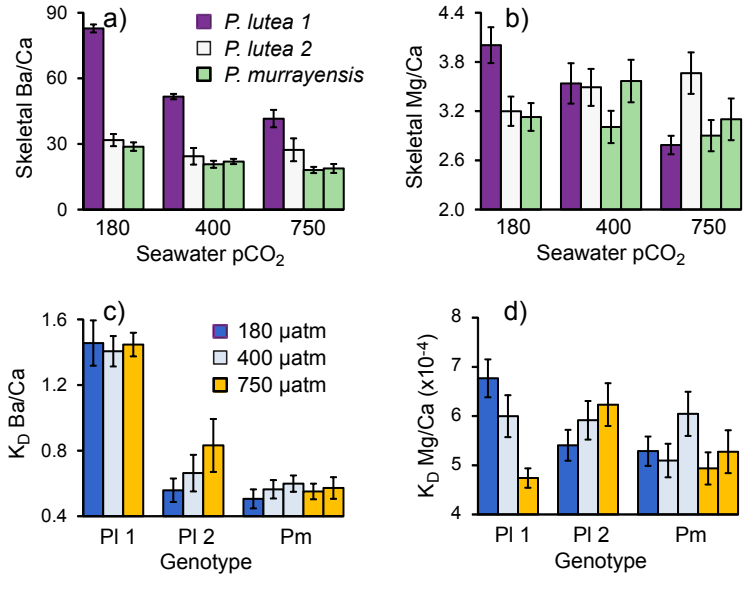

Figure 3. Relationships between coral skeletal $K_D$ Ba/Ca and Mg/Ca and calcification, photosynthesis and respiration in each coral genotype. Error bars indicate typical 95% confidence limits for $K_D$ (calulated by compounding 95% confidence limits for skeletal Me/Ca and seawater Me/Ca, where Me is Mg or Ba) and one standard deviation for physiological measurements.

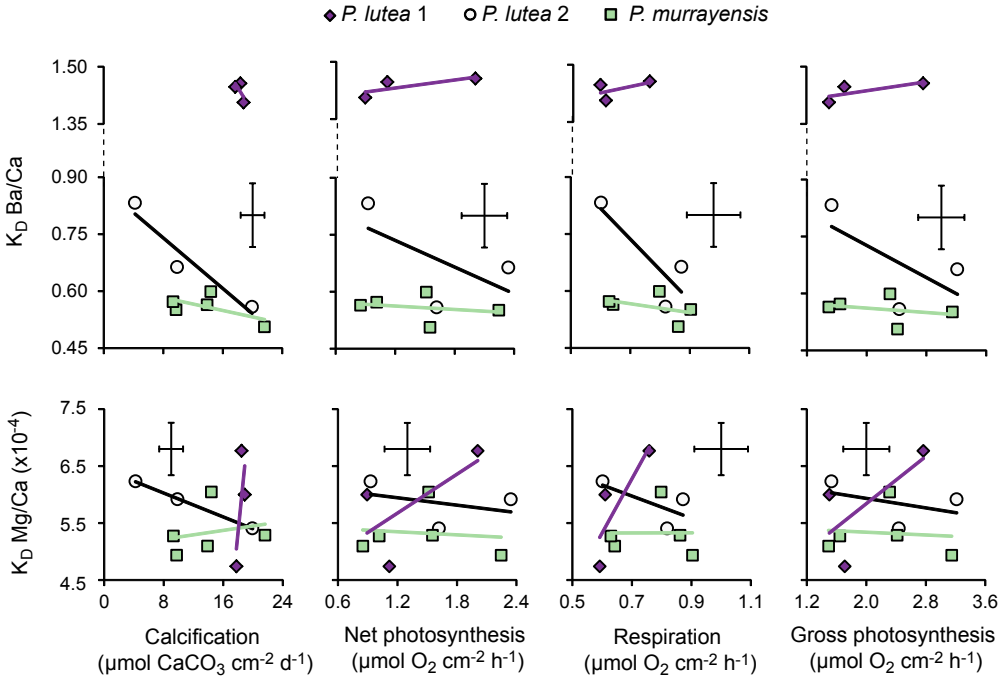


Figure 4. Covariations between a) $K_D$ Ba/Ca and $K_D$ Mg/Ca (both this study), b) $K_D$ Ba/Ca and $K_D$ Sr/Ca (Cole et al., 2016) and c) $K_D$ Mg/Ca and $K_D$ Sr/Ca of each individual coral. Regressions are grouped per coral genotype. Error bars indicate typical 95% confidence limits for $K_D$ (calculated by compounding 95% confidence limits for skeletal and seawater Me/Ca).

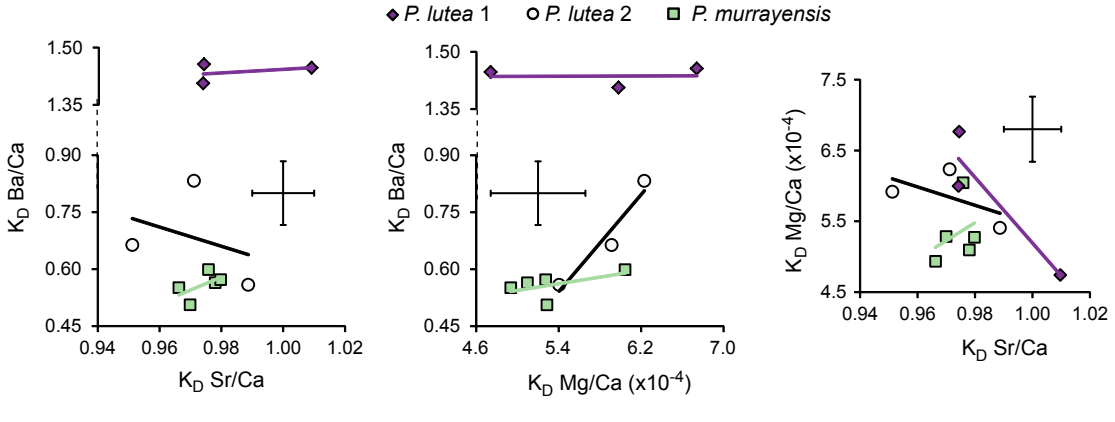

Table A1. Seawater and skeletal Ba/Ca and Mg/Ca data. Values are means ± standard deviation (n). Duplicate colonies of *P. murrayensis* at 400 and 750 µatm are denoted a and b.

| Seawater $pCO_2$ | Seawater concentrations | | Genotype | Skeletal concentrations | |
|---|---|---|---|---|---|
| | Ba/Ca | Mg/Ca | | Ba/Ca | Mg/Ca |
| | µmol $mol^{-1}$ | mol $mol^{-1}$ | | µmol $mol^{-1}$ | mmol $mol^{-1}$ |
| 180 µatm | 56.9 ± 4.6 (5) | 5.92 ± 0.08 (5) | *P. lutea 1* | 82.1 ± 5.1 (41) | 4.004 ± 0.219 (41) |
| | | | *P. lutea 2* | 28.5 ± 1.2 (29) | 3.199 ± 0.178 (29) |
| | | | *P. murrayensis* | 28.8 ± 5.8 (36) | 3.128 ± 0.169 (36) |
| 400 µatm | 36.7 ± 2.0 (5) | 5.90 ± 0.08 (5) | *P. lutea 1* | 51.6 ± 3.2 (26) | 3.538 ± 0.246 (26) |
| | | | *P. lutea 2* | 24.4 ± 9.2 (23) | 3.490 ± 0.225 (23) |
| | | | *P. murrayensis a* | 20.7 ± 3.9 (23) | 3.007 ± 0.196 (23) |
| | | | *P. murrayensis b* | 22.0 ± 2.7 (20) | 3.567 ± 0.259 (20) |
| 750 µatm | 32.8 ± 0.9 (5) | 5.88 ± 0.05 (5) | *P. lutea 1* | 47.5 ± 4.4 (24) | 2.786 ± 0.113 (24) |
| | | | *P. lutea 2* | 27.3 ± 12.0 (21) | 3.663 ± 0.253 (21) |
| | | | *P. murrayensis a* | 18.2 ± 2.8 (15) | 2.901 ± 0.191 (15) |
| | | | *P. murrayensis b* | 18.8 ± 3.6 (12) | 3.100 ± 0.254 (12) |